

19th December 2009

Carbon Nanoparticle Surface Functionalisation: Converting Negatively Charged Sulphonate to Positively Charged Sulphonamide

John D. Watkins,^a Ruth Lawrence,^a James E. Taylor,^a Steven D. Bull,^a Geoff Nelson,^b
John S. Foord,^b Daniel Wolverson,^c Liza Rassaei,^a Nick D.M. Evans,^d Silvia Antón
Gascon,^d and Frank Marken^{a*}

^a *Department of Chemistry, University of Bath, Bath BA2 7AY, UK*

^b *Chemistry Research Laboratories, Oxford University, Oxford OX1 3TA, UK*

^c *Department of Physics, University of Bath, Bath BA2 7AY, UK*

^d *Department of Chemistry, Loughborough University, Leics, LE11 3TU, UK*

To be submitted to PCCP

Proofs to F. Marken

Email f.marken@bath.ac.uk

Abstract

The surface functionalities of commercial sulphonate-modified carbon nanoparticles (ca. 9-18 nm diameter, Emperor 2000) have been converted from negatively charged to positively charged via sulphonylchloride formation followed by reaction with amines to give sulphonamides. With ethylenediamine, the resulting positively charged carbon nanoparticles exhibit water solubility (in the absence of added electrolyte), a positive zeta-potential, and the ability to assemble into insoluble porous carbon films via layer-by-layer deposition employing alternating positive and negative carbon nanoparticles. Sulphonamide-functionalised carbon nanoparticles are characterised by Raman, AFM, XPS, and voltammetric methods. Stable thin film deposits are formed on 3 mm diameter glassy carbon electrodes and cyclic voltammetry is used to characterise capacitive background currents and the adsorption of the negatively charged redox probe indigo carmine. The Langmuirian binding constant $K = 4000 \text{ mol}^{-1}\text{dm}^3$ is estimated and the number of positively charged binding sites per particle determined as a function of pH.

Key Words: voltammetry, carbon nanoparticles, adsorption, thin film, modified surface, sulphonamide, layer-by-layer, surface immobilisation, sensor.

1. Introduction

Nano-carbon based electrodes e.g. based on carbon nanotubes,^{1,2} carbon nanofibers,³ grapheme,⁴ or carbon nanoparticles⁵ are of interest in electrochemical processes due to their often highly active surface characteristics⁶ and their ease of functionalisation.^{7,8} Carbon nanoparticles are of particular interest in sensing applications.⁹ A solvent evaporation based deposition method for negatively charged Emperor 2000 carbon nanoparticles in combination with a positively charged chitosan binding agent has been proposed for the formation of stable carbon nanoparticle films on glassy carbon electrodes.¹⁰ It has also been shown that a layer-by-layer deposition process allows carbon nanoparticles to be deposited onto tin-doped indium oxide (ITO) electrodes using a poly-(diallyldimethylammonium chloride)¹¹ or chitosan¹² binder.

The introduction/modification of functional groups at carbon surfaces provides an important tool for achieving chemical selectivity or a high level of charge at the surface.¹³ The oxidative treatment of carbons is known to introduce negative surface functionalities.¹⁴ Diazonium salt chemistry, either spontaneous^{15,16,17} or electrochemically assisted,¹⁸ has been widely applied for the introduction of various types of surface functionalities. Also the Kolbe-decarboxylation of carboxylates has been used to functionalise carbon electrode surfaces.¹⁹

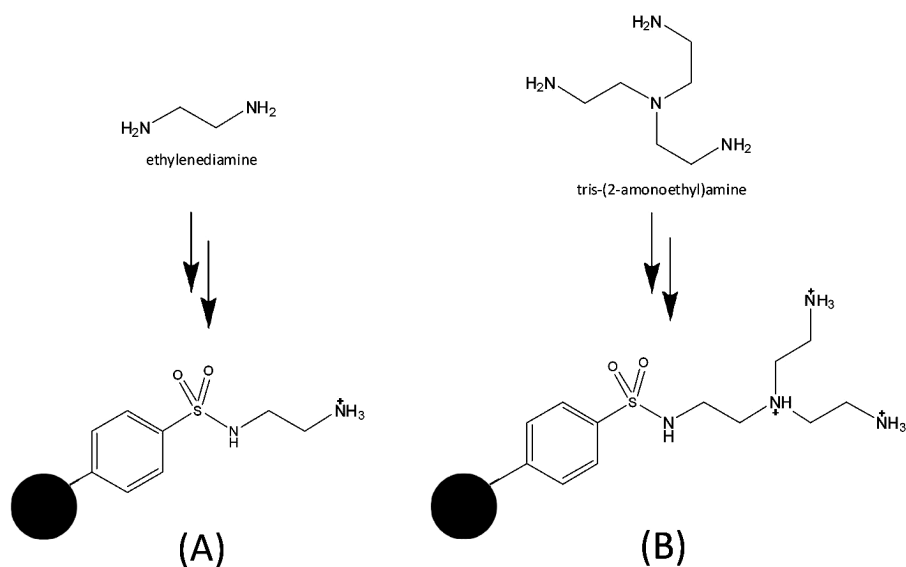


Figure 1. Two amines tested for attachment to the sulphonyl functional group of the carbon nanoparticles and the expected surface functionalised products.

In this study sulphonate-functionalized carbon nanoparticles (Emperor 2000, Cabot Corporation) are employed as a precursor material. These nanoparticles possess negatively charged sulphonate functional groups which can be modified by attaching amines to give sulphonamides with single or multiple positive charges (see Figure 1). The resulting particles are complementary in charge to the Emperor 2000 precursor particles and of interest in a wide range of sensor and electrode modification application. It is shown here that the positively charged particles bind to negatively charged silica surfaces and that a combination of positive and negative carbon nanoparticles can assemble into novel nano-composites of mixed surface charge. The anionic redox probe indigo carmine is shown to bind electrostatically to the positively charged carbon particles, which allows characterisation of surface properties as a function of pH.

2. Experimental

2.1. Reagents

Emperor 2000 carbon nanoparticles used as the starting material were obtained from Cabot Corporation. Other reagents were used without further purification: sodium nitrate (Sigma Aldrich, 99.0%), indigo carmine, certified (Aldrich), acetic acid (Aldrich, 99.7+%), ortho-phosphoric acid (Fisher Scientific), boric acid (Aldrich, $\geq 99.5\%$). Britton-Robinson buffer was prepared from 0.04M of each of boric acid, phosphoric acid, and acetic acid and adjusting with sodium hydroxide to the desired pH. Demineralised and filtered water was taken from a Thermo Scientific water purification system (Barnstead Nanopure) with not less than 18.2 M Ω cm resistivity. Experiments were conducted at $20 \pm 2^\circ\text{C}$.

2.2. Instrumentation

For voltammetric studies a microAutolab III potentiostat system (EcoChemie, Netherlands) was employed with a Pt gauze counter electrode and a saturated calomel (SCE) reference electrode (Radiometer, Copenhagen). Atomic force microscopy (AFM) was conducted in tapping mode under ambient conditions using a Nanoscope IIIA (V6.14) and a Nanosensors NCH-16 tip. Raman spectroscopy studies were carried out with a Renishaw Raman microscope system with a resolution of about 2 cm^{-1} and using an excitation energy of 5.08 eV (244 nm) provided by a frequency-doubled continuous-wave argon ion laser (reference diamond = 1332 cm^{-1}). X-ray

photoelectron spectroscopy (XPS) was conducted using a VSW hemispherical analyser, excited using a monochromatic Al K α X-ray source at 1486.6eV. Spectra were background corrected using a Shirley background scan and peak fitting was conducted using the XPSPEAK (ver. 4.1) software package. A Malvern Zetamaster S (Malvern Instruments) was used for zeta potential measurements. Each sample was measured 10 times, and each of these measurements took ca. 30 seconds.

2.3. Procedure I.: Surface Modification of Carbon Nanoparticles

For step (A) (see Figure 2) typically 1 g of carbon nanoparticles (Emperor 2000) were sonicated in dry dichloromethane in a round bottom flask for 30 minutes. The flask was degassed with nitrogen gas at 0°C and 10 cm³ of thionyl chloride was added dropwise under continuous stirring. The flask was then allowed to warm to room temperature whilst stirring for 2-3 hours. Excess thionyl chloride and solvent were removed by rotary evaporation.

For Step (B) (see Figure 2) 10 cm³ of ethylene diamine was added into a 250 cm³ round bottom flask with 30 cm³ of dry dichloromethane and the temperature cooled to 0°C. The sulphonylchloride functionalised carbon nanoparticles were added in small portions, and then the reaction was allowed to warm to room temperature whilst stirring for 2 hours. Excess amine and dichloromethane were removed by rotary evaporation. Aqueous 1 M HCl was then added and a black solid was collected by Büchner filtration.

2.4. Procedure II.: Deposition of Carbon Nanoparticle Films Onto Glassy Carbon Electrodes

For deposition 3.5 mg of the sulphonamide-functionalised nanoparticles were added into 1.5 cm³ distilled water. The resulting solution/suspension was initially sonicated for 1 hour and then shaken vigorously prior to each use. Aliquots of this solution/suspension were pipetted directly onto a clean 3 mm diameter glassy carbon electrode and allowed to evaporate at 80°C in an oven. The resulting film exhibited good adhesion to glassy carbon and was used directly in further experiments.

2.5. Procedure III.: Indigo Carmine Adsorption into Carbon Nanoparticle Films

For modification by indigo carmine the carbon nanoparticle films on glassy carbon electrodes (see above) were dipped into solutions of indigo carmine in distilled water of varying concentration and left to equilibrate for 5 minutes. The electrodes were then rinsed with distilled water and placed into aqueous 1 M sodium nitrate for electrochemical experiments.

3. Results and Discussion

3.1. Synthesis and Characterisation of Sulphonamide-Modified Carbon Nanoparticles

Precursor carbon nanoparticles in this study are sulfonate-modified “Emperor 2000” particles with ca. 9 to 18 nm diameter.²⁰ These negatively charged particles are readily soluble in aqueous media and they have been employed in nanoparticle deposition processes with positively charged poly-electrolyte binders.²¹ The key idea for this study is based on the conversion of the sulfonate into sulfonyl chloride end-groups which are then functionalised with amine functionalities (see Figure 1) to provide a positively charged carbon nanoparticle complementary in charge to the original Emperor 2000 particle but identical in size.

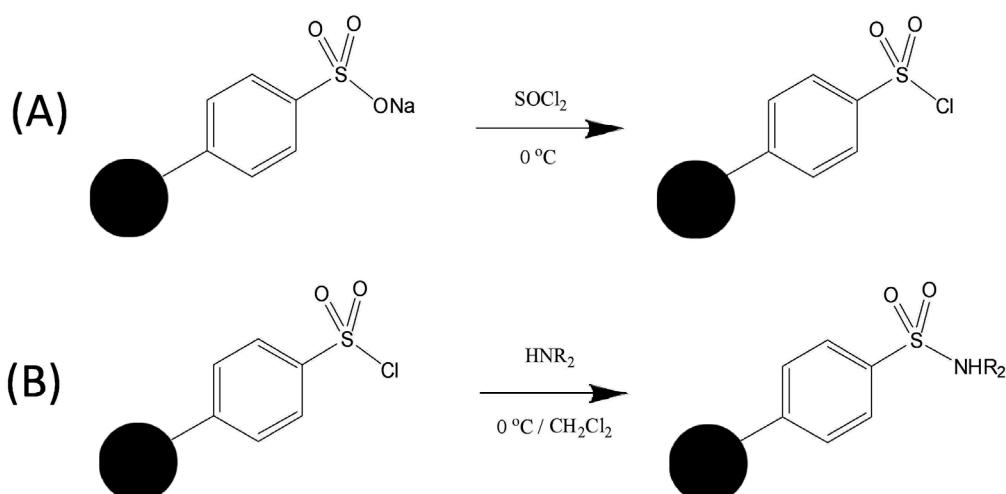


Figure 2. (A) Conversion of sulphonate to sulphonylchloride with thionylchloride at 0°C. (B) Formation of sulphonamide by reacting sulphonylchloride with amine at 0°C in dichloromethane.

It was expected that the ethylene diamine derivative would lead to a number of positive surface charges equivalent to the number of negative charges on the Emperor 2000 precursor nanoparticles. Theoretically, for the tris-(2-aminoethyl)amine derivative a three times higher surface charge would be possible (see Figure 1). The ethylene diamine derivatised nanoparticles were obtained as black powder and they slowly dissolved into pure water to give dark-yellow solutions of low concentration. After sonication a black solution/suspension of 2.3 mg per cm³ was obtained and this was employed for deposition onto electrode surfaces. The tris-(2-aminoethyl)amine derivatised nanoparticles appeared completely insoluble in water (possibly due to stronger interaction between particles). In the presence of buffer or electrolyte both types of amine derivatised carbon nanoparticles remained completely water-insoluble and resisted homogenisation.

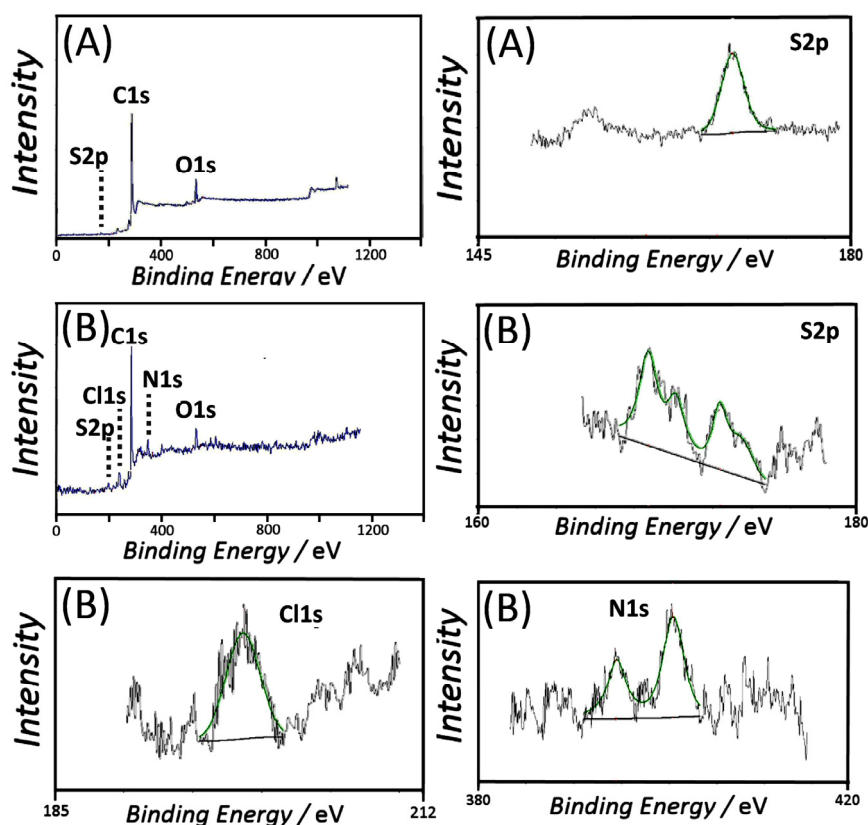


Figure 3. XPS data for (A) Emperor 2000 nanoparticles and (B) ethylenediamine sulphonamide functionalised nanoparticles.

Surface composition characterisation of the modified carbon nanoparticles was achieved by x-ray photoelectron spectroscopy (XPS). Figure 3 shows survey scans for (A) Emperor 2000 particles and (B) ethylene diamine derivatised particles. It can be seen that Emperor 2000 material has no nitrogen functionalities (no N1s signal). In contrast, the ethylene diamine derivative shows a pair of N1s peaks (possibly protonated and un-protonated amine). The sulphur peak (S2p) appears to be split in the ethylene diamine derivative possibly indicating some protonation of the sulphonamide. From the ratio of the sulphur S2p peak at ca. 169.4 eV and nitrogen N1s peak at ca. 394.5 eV a roughly 2 : 1 nitrogen to sulphur ratio is estimated. A

chlorine peak (Cl1s) is likely to be linked to chloride counter anions associated with the protonated surface amine.

The presence of amine functionalities is further supported by zeta potential data obtained in pure water which show that Emperor 2000 nanoparticles in solution exhibit a zeta potential of ca. -44.5mV whereas the ethylene diamine derivatised sulphonamide nanoparticles exhibit a zeta potential of ca. +29.8mV. Raman spectroscopy (see Figure 4A) is not surface sensitive but does provide a well defined G mode peak at 1576 cm^{-1} (expected for graphite 1581 cm^{-1} ²²) consistent with a ordered graphitic material with a low level of defects.

Due to the positive surface charge ethylene diamine derivatised nanoparticles show different adsorption behaviour compared to negatively charged Emperor 2000 particles. For example, ethylene diamine derivatised particles (in contrast to Emperor 2000) readily adsorb onto glass (or silica) slides. When a first layer of the positively charged carbon nanoparticles has been applied alternating dip and rinse cycles using negatively and positively charged carbon nanoparticles in water can be used to build up carbon nano-composite deposits. These layer-by-layer deposits become visible to the naked eye after ca. 20 to 40 deposition cycles. An AFM image of a 20-layer deposit is shown in Figure 4B. Globular deposits with 40-50 nm height can be observed.

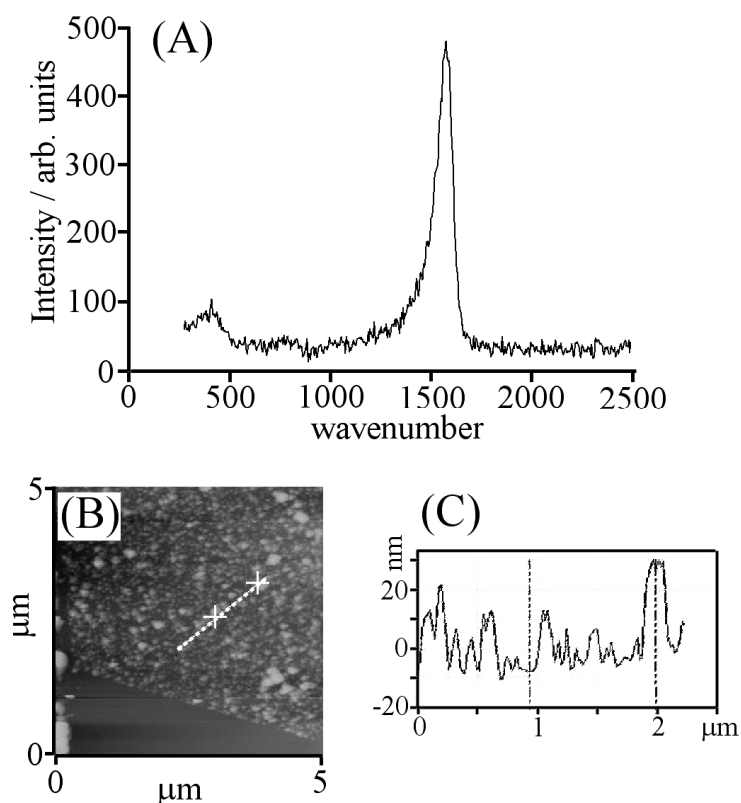


Figure 4. (A) Raman spectrum (I) for ethylenediamine sulphonamide functionalised nanoparticles and (B,C) AFM image and profile for a 20-layer film formed by alternating deposition of positively and negatively charged carbon nanoparticles

3.2. Voltammetric Characterisation of Carbon Nanoparticle Sulphonamides I.:

Capacitive Charging

Initially cyclic voltammograms were obtained for films of ethylene diamine derivatised nanoparticles deposited onto glassy carbon substrate electrodes (see Experimental). The capacitive current response was measured as a function of the amount of applied carbon nanoparticles in aqueous 1 M sodium nitrate. Data in

Figure 5A shows well-defined capacitive current responses over a potential range from 0.0 V to -0.8 V vs. SCE.

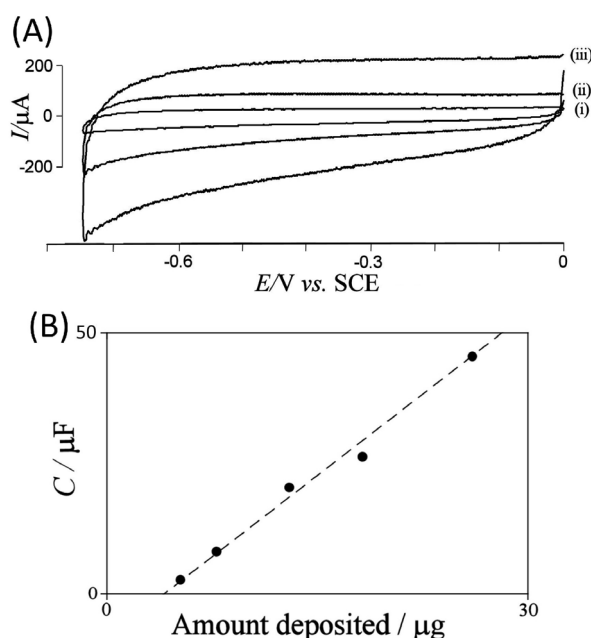
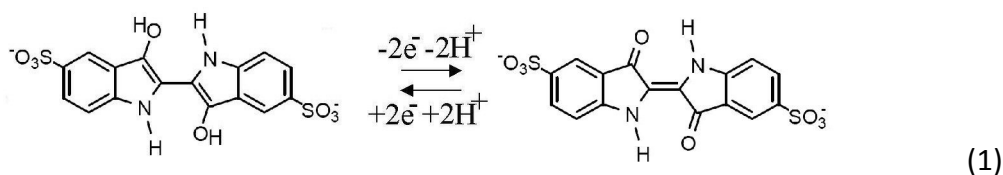


Figure 5. (A) Cyclic voltammograms (scan rate 100 mVs^{-1}) obtained for films of (i) 4.6 μg , (ii) 7.0 μg , and (iii) 11.7 μg ethylene diamine derivatised nanoparticles deposited onto a 3 mm diameter glassy carbon electrode and immersed into aqueous 1 M NaNO_3 . (B) Plot of the capacitance (at -0.3 V vs. SCE) versus mass of carbon nanoparticles.

A linear relationship between the capacitance and the amount of deposited carbon material is observed (see Figure 5B) and the resulting specific capacitance is 3.3 Fg^{-1} . The tris-(2-aminoethyl)amine derivatised carbon nanoparticles exhibit the same type of capacitive charging currents (not shown) with essentially identical specific capacitance. This specific capacitance is consistent with that observed for other types of nano-carbon materials.²³

3.3. Voltammetric Characterisation of Carbon Nanoparticle Sulphonamides II.: Adsorption and Redox Cycling of Indigo Carmine

The terminating amine present at the surface of the carbon nanoparticle was expected to be protonated over most of the aqueous pH range. Experiments were therefore conducted by adsorbing the anionic redox probe indigo carmine²⁴ into the positively charged carbon host followed by voltammetry in aqueous 1 M NaNO₃. Indigo carmine is a water soluble molecule with a well defined two-electron two-proton reversible reduction (see equation 1) with a reversible potential of -0.43 V vs. SCE at pH 7.^{25,26}



Electrodes were modified first with a film of sulphonamide-functionalised carbon nanoparticles and then immersed into an adsorption solution of indigo carmine in water (see Experimental). After adsorption of indigo carmine for 5 minutes and careful rinsing with 1 M NaNO₃, voltammetric measurements were conducted in aqueous 1 M NaNO₃. Voltammograms shown in Figure 6A are typical for a surface immobilised indigo carmine and show good reversibility and relatively good stability over multiple potential cycles. The signal remains clearly visible up to 20 consecutive scans (not shown). The scan rate dependence of the peak current shows direct proportionality which is characteristic for a surface immobilised redox species.

Therefore, the charge under the peaks is directly representative of the amount of indigo carmine immobilised at the carbon nanoparticle electrode. Varying the concentration of the indigo carmine dipping solution allows the construction of a Langmuir-type adsorption isotherm (see Figure 6D). From this plot of anodic charge versus indigo carmine concentration an estimate of the binding coefficient and number of active binding sites can be gained. The binding constant is estimated as $K = 4000 \text{ mol}^{-1}\text{dm}^3$ and compares favourably to the previously observed values for carbon nano-composites with chitosan binder and Emperor 2000 nanoparticles.¹⁰ The tris-(2-aminoethyl)amine derivatised carbon nanoparticles formed more uneven deposits (from a 50:50 water:ethanol mixture) and were tested in a similar way (data not shown). The Langmuirian binding constant was estimated to be essentially identical to that for the ethylene diamine derivatised particles. The charge under the peak was not significantly higher which suggests that the tris-(2-aminoethyl)amine derivatised carbon nanoparticles may be chemically less well defined without the anticipated increase in positive charges. There could be multiple sulphonamide bonds of tris-(2-aminoethyl)amine to the surface causing less free amine functionality.

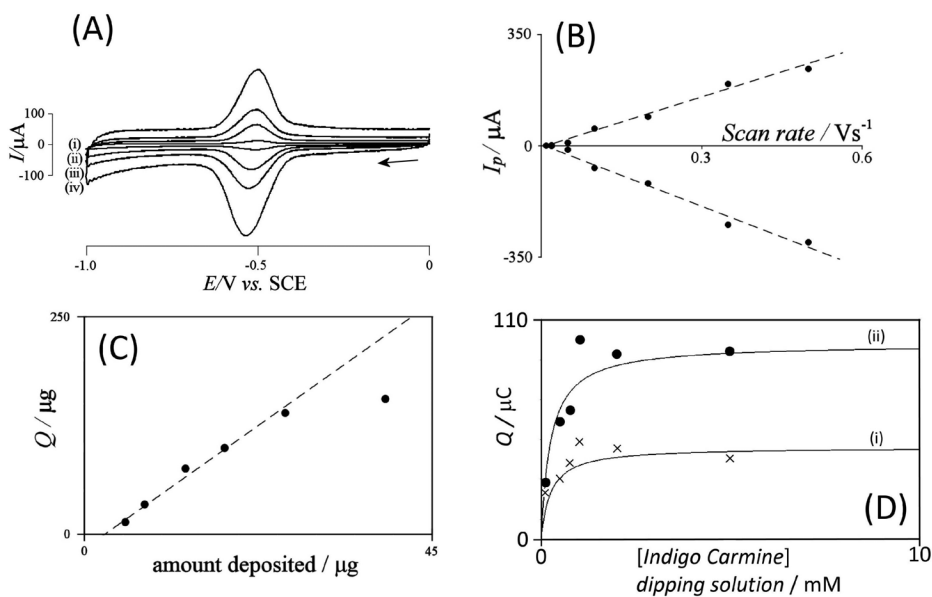


Figure 6. (A) Cyclic voltammograms (scan rate (i) 50 mVs^{-1} , (ii) 100 mVs^{-1} , (iii) 200 mVs^{-1} , and (iv) 500 mVs^{-1}) obtained with a deposit of $7 \mu\text{g}$ of ethylene diamine derivatised carbon nanoparticles at a 3 mm diameter glassy carbon electrode in 1 M NaNO_3 (after dipping into 1 mM indigo carmine for 5 minutes). (B) Plot of anodic peak current for indigo carmine reduction versus scan rate. (C) Plot of the anodic peak charge for indigo carmine reduction versus amount of carbon nanoparticles deposited. (D) Plots of the anodic peak charge for indigo carmine reduction versus the concentration in the indigo carmine dipping solution for (i) $7 \mu\text{g}$ and (ii) $16 \mu\text{g}$ carbon nanoparticle deposit.

From the indigo carmine adsorption limit (see Figure 6D) it is possible to estimate the number of cationic binding sites per carbon nanoparticle. The distribution of carbon nanoparticle diameters is $9 - 18 \text{ nm}$, but it is possible to use the modal average of 12 nm , and thus by using the approximate density of the carbon nanoparticles 2.2 gcm^{-3} , it is possible to calculate a charge (or active binding sites) of typically $600-700$ per carbon nanoparticle. This results in a realistic molecular “foot-print” per sulphonamide of 75 \AA^2 .

3.4. Voltammetric Characterisation of Carbon Nanoparticle Sulphonamides III.: pH Effects on the Redox Cycling of Indigo Carmine

Since the protonation of the terminating amine groups on the carbon nanoparticles is essential for the electrostatic binding properties of the surface, the effect of pH was analysed next. Figure 7A shows typical voltammetric responses obtained at acidic and alkaline pH. Both, the peak position and the magnitude of peak currents can be seen to vary systematically. Even up to pH 13 a reversible signal for indigo carmine reduction is clearly observed, however, the charge under the peak is diminished (see Figure 7C). The effect of the pH on the adsorption of indigo carmine is shown in Figure 7B. It was observed that between ca. pH 4 and pH 8 there was no significant change in the surface concentration of indigo carmine. However, at lower pH the charge under the voltammetric peaks is increasing possibly due to the additional protonation of sulphonamide. At more alkaline pH values the number of cationic binding sites decreases. The transition to lower binding appears to occur around pH 9 suggesting that the pKa of the surface bound terminating amine groups is approximately 9. However, the transition is very broad and deprotonation incomplete even in more alkaline conditions which may indicate some interaction.

An approximate Nernstian shift was observed for the midpoint potential (see Figure 7B). The gradient for this Nernstian shift is ca. 59 mV for pH 2 to pH 7. After this the gradient is ca. 30 mV for pH 7 to pH 13. This change in gradient is indicative of the reduced form of indigo carmine becoming deprotonated and the electrochemical process changing from a $2e^-/2H^+$ (pH 2 to pH 7) to a $2e^-/1H^+$ (pH 7 to pH 13) process.

The pKa of *leuco*-indigo carmine can thus be estimated to be about 7.7 which is very close to literature value for the pKa of *leuco*-indigo carmine (pKa = 8.0).²⁷

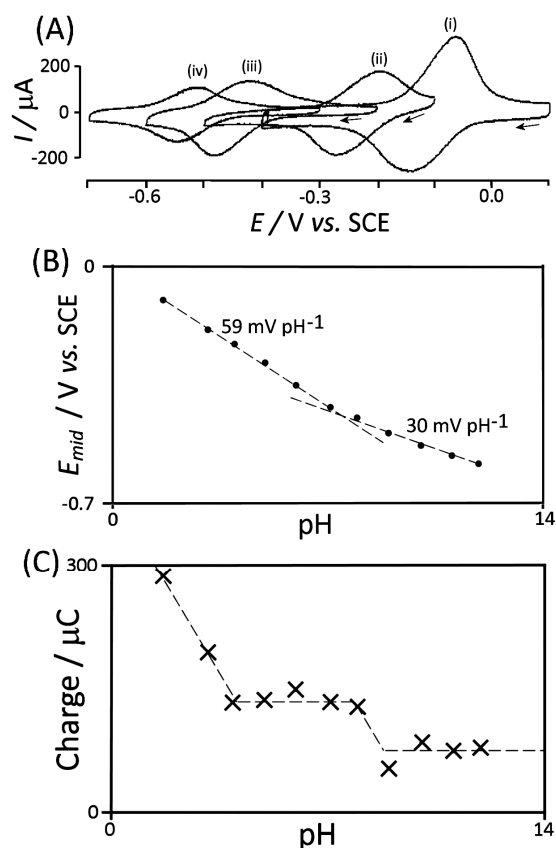


Figure 7. (A) Cyclic voltammograms (scan rate of 100mVs^{-1}) for the reduction of indigo carmine (adsorbed from 1 mM solution of indigo carmine in Britton-Robinson buffer onto $16 \mu\text{g}$ carbon nanoparticles at a 3 mm diameter glassy carbon electrode) immersed in 0.12 M Britton-Robinson at pH (i) 2, (ii) 4, (iii) 8, and (iv) 10. (B) Plot of the midpoint potential ($E_{\text{mid}} = \frac{1}{2} E_{\text{p}}^{\text{ox}} + \frac{1}{2} E_{\text{p}}^{\text{red}}$) versus pH. (C) Plot of the anodic charge for the indigo carmine reduction versus pH.

4. Conclusions

A versatile synthetic procedure for the preparation for sulphonamide functionalised carbon nanoparticles has been described. The functionalised nanoparticles have been characterised by x-ray photoelectron spectroscopy and zeta potential measurements showing that the amine functionalised particle exhibit a positive surface charge in aqueous solution at neutral pH. The positively charged carbon nanoparticles have been employed (i) for assembly onto glass surfaces and (ii) to electrostatically bind redox active indigo carmine anions. The binding process was studied using cyclic voltammetry. The number of binding sites was estimated to be 600-700 per nanoparticle and the Langmuirian binding constant for indigo carmine is ca. $4000 \text{ mol}^{-1}\text{dm}^3$.

5. Acknowledgements

J.D.W. and L.R. thank the EPSRC for financial support.

References

- 1 M. Pumera, *Chem. Eur. J.* 2009, **15**, 4970.
- 2 C.E. Banks and R.G. Compton, *Anal. Sci.* 2005, **21**, 1263.
- 3 L. Rassaei, M. Sillanpää, M.J. Bonné and F. Marken, *Electroanal.* 2007, **19**, 1461.
- 4 J.F. Wang, S.L. Yang, D.Y. Guo, P. Yu, D. Li, J.S. Ye and L.Q. Mao, *Electrochem. Commun.* 2009, **11**, 1892.
- 5 L. Vidal, A. Chisvert, A. Canals, E. Psillakis, A. Lapkin, F. Acosta, K.J. Edler, J.A. Holdaway and F. Marken, *Anal. Chim. Acta* 2008, **616**, 28.
- 6 C.E. Banks and R.G. Compton, *Analyst* 2006, **131**, 15.
- 7 F. Barriere and A.J. Downard, *J. Solid State Electrochem.* 2008, **12**, 1231.
- 8 G.G. Wildgoose, C.E. Banks, H.C. Leventis and R.G. Compton, *Microchim. Acta* 2006, **152**, 187.
- 9 K. Szot, A. Lesniewski, J. Niedziolka, M. Jonsson, C. Rizzi, L. Gaillon, F. Marken, J. Rogalski and M. Opallo, *J. Electroanal. Chem.* 2008, **623**, 170.
- 10 L. Rassaei, M. Sillanpää and F. Marken, *Electrochim. Acta* 2008, **53**, 5732.
- 11 M. Amiri, S. Shahrokhian and F. Marken, *Electroanal.* 2007, **19**, 1032.
- 12 L. Rassaei, M.J. Bonné, M. Sillanpää and F. Marken, *New J. Chem.* 2008, **32**, 1253.
- 13 P. Abiman, G.G. Wildgoose, A. Crossley and R.G. Compton, *J. Mater. Chem.* 2008, **18**, 3948.
- 14 M. Wang, N. Simon, C. Decorse-Pascanut, M. Bouttemy, A. Etcheberry, M.S. Li, R. Boukherroub and S. Szunerits, *Electrochim. Acta* 2009, **54**, 5818.

-
- 15 M. Toupin and D. Belanger, *Langmuir* 2008, **24**, 1910.
- 16 M. Pandurangappa, N.S. Lawrence and R.G. Compton, *Analyst* 2002, **127**, 1568.
- 17 J.M. Seinberg, M. Kullapere, U. Maeorg, F.C. Maschion, G. Maia, D.J. Schiffrin and K. Tammeveski, *J. Electroanal. Chem.* 2008, **624**, 151.
- 18 A.J. Downard, *Electroanal.* 2000, **12**, 1085.
- 19 C.P. Andrieux, F. Gonzalez and J.M. Savéant, *J. Amer. Chem. Soc.* 1997, **119**, 4292.
- 20 M. Amiri, S. Shahrokhian, E. Psillakis and F. Marken, *Anal. Chim. Acta* 2007, **593**, 117.
- 21 L. Rassaei, M. Sillanpää, K.J. Edler and F. Marken, *Electroanal.* 2009, **21**, 261.
- 22 A.C. Ferrari and J. Robertson, *Phys. Rev. B.* 2000, **61**, 14095.
- 23 F. Marken, M.L. Gerrard, I.M. Mellor, R.J. Mortimer, C.E. Madden, S. Fletcher, K. Holt, J.S. Foord, R.H. Dahm and F. Page, *Electrochem. Commun.* 2001, **3**, 177.
- 24 L. Rassaei, M.J. Bonné, M. Sillanpää and F. Marken, *New J. Chem.* 2008, **32**, 1253.
- 25 S.C. Mo, J.M. Na, H. Mo and L. Chen, *Anal. Lett.*, 1992, **25**, 899.
- 26 Y.J. Li and S.J. Dong, *J. Electroanal. Chem.* 1993, **348**, 181.
- 27 A.M. Bond, F. Marken, E. Hill, R.G. Compton and H. Hügél, *J. Chem. Soc. Perkin Trans. 2*, 1997, 1735 and references cited therein.